J Appl Electrochem (2009) 39:159–166
DOI 10.1007/s10800-008-9659-3

ORIGINAL PAPER

Development of MnO_2-incorporated high performance aluminum alloy matrix sacrificial anodes

S. M. A. Shibli · K. K. Binoj

Received: 23 November 2007 / Accepted: 17 May 2008 / Published online: 18 September 2008
© Springer Science+Business Media B.V. 2008

Abstract Manganese dioxide, a potential catalyst in many electrochemical reactions, was explored as an effective activator in Al + 5% Zn alloy sacrificial anodes. The catalytic influence of MnO_2 on the anodes was microstructurally and electrochemically characterized using different electrochemical techniques. The process of incorporation of MnO_2 not only improved the grain size but also the galvanic performance of the anodes significantly. A galvanic performance as high as 80% was achieved by incorporating an optimum quantity (0.5%) of MnO_2 in the anode matrix. High and steady active open circuit potential, very low polarization and substantial reduction in self corrosion were achieved during galvanic exposure tests. Effective activation of the anodes by MnO_2 was also revealed by the results of electrochemical impedance analysis. The tolerance to biofouling on the anode surface was studied by quantifying the number of micro-organisms on the anode surface after immersing in natural sea water containing the micro-organisms.

Keywords Manganese dioxide · Aluminum · Sacrificial anode · Corrosion · Pitting

1 Introduction

Aluminum and aluminum alloys are extensively used as sacrificial anodes as they have undeniable economic advantages in view of their merits such as low density, high current capacity and reasonable cost. Aluminum is the most commonly used sacrificial material for cathodic protection of steel in sea water [1, 2]. However, pure aluminum forms a passive film on its surface at an open circuit potential of about −0.800 V versus SCE in sea water [3, 4], which make it useless as a sacrificial anode in cathodic protection of steel in sea water. This film is relatively stable in aqueous solutions over a wide pH range of 4.0–8.5 [5]. The passivity of aluminum can be overcome by adding suitable alloying elements such as In, Hg, Ga, Sn, Bi [6–11]. However, most of these metal activated sacrificial anodes undergo pitting corrosion in chloride environments.

Zinc has an effect of propagation and re-passivation of metastable pits in Al–Zn alloy. Higher amounts of zinc causes stable pitting, while lower amounts results in poor aluminum activation. Muller and Galvele [12, 13], have reported that the alloying of aluminum with 5% zinc results in high aluminum activation without substantial pit formation. The addition of 5% zinc to aluminum is the optimum that leads to significant improvement in metallurgical and electrochemical characteristics of the alloy through formation of β phase [14]. The same alloy composition was also selected for the present work.

Metal oxides play a versatile and important role in heterogeneous catalysis, gas sensors and corrosion. Aluminum matrix composites exhibit higher specific strength, specific modulus and wear resistance when compared to unreinforced alloys [15–19]. The inclusion of metal oxides can improve the grain boundaries, suppressing grain boundary corrosion. The oxides of Al and Mn have been used for the fabrication of high wear resistance sacrificial anodes [20–22]. Similarly SiO_2, ZrO_2 and CeO_2 have been used to reinforce the Al matrix [23, 24]. The inclusion of Al_2O_3 in aluminum alloys can result in substantial metallurgical improvement [25]. Zinc oxide nano particles can also be used for the effective activation of

S. M. A. Shibli (✉) · K. K. Binoj
Department of Chemistry, University of Kerala, Kariavattom Campus, Trivandrum 695 581, Kerala, India
e-mail: smashibli@yahoo.com

Al–Zn sacrificial anodes [26]. The effect of TiO_2 has been little investigated since 1970 though its role in fabricating dimensionally stable electrodes is well established [27, 28].

MnO_2 has traditionally received a lot of attention due to its widespread use in industrial electrochemistry as it has desirable chemical and electrochemical characteristics [29]. MnO_2 is the most common positive electrode material used in power sources. It is also extensively used as an efficient catalyst and as a pseudo capacitor due to its good electrochemical performance, environmental acceptability and low cost [30–33]. It has been reported that the incorporation of MnO_2 into an aluminum matrix significantly improves both hardness and wear resistance [34, 35]. Though some investigations have been made to improve the mechanical and micro/macro structural characteristics of aluminum alloy by MnO_2 incorporation [15, 34], no one has dealt with activation of Al–Zn alloy sacrificial anodes. In this context the present study explores and evaluates the catalytic effect of MnO_2 for the effective activation of Al–Zn sacrificial anodes in marine environments.

2 Experimental methods

2.1 Fabrication of the anode

Commercially available pure aluminum (99.90%) and zinc (99.95%) ingots were used for casting Al + 5% Zn alloy anodes. The required quantities of the metal ingots were heated in a graphite crucible in a muffle furnace. A silicon carbide rod was used for homogenization of the melt. The melt at 725 ± 10 °C was poured into a graphite die having dimensions 4 × 2 × 0.3 cm. The cast anodes were polished by using different grades of emery paper down to 300, degreased with trichloroethylene and dried by blowing hot air at 60 °C. For the fabrication of the MnO_2-incorporated anodes, the required amount of MnO_2 (Merck India, assay-99.0%) was added to the melt with sufficient stirring and reheated again before casting the Al + 5% Zn alloy anode.

2.2 Physicochemical characterization

A Hitachi S-2400 instrument was used to record scanning electron micrographs of the anode surface. The metallographic samples for SEM analysis were cut from the centre of the bulk anode. They were finely ground and polished to the required extent. During the polishing stage, the metal was protected from galvanic deterioration by means of dehydrated ethanol for lubrication and cleaning. The samples were etched with 5% NaOH solution, washed with distilled water and examined by secondary electron signal.

The hardness of the anodes was determined as per ASTM 384-89 by using a Vickers micro hardness indenter. The hardness values were measured at different places on each anode and the average values were recorded. The standard deviation was found to be less than five units in any case.

2.3 Electrochemical evaluation

2.3.1 OCP and CCP variation

The open circuit potential (OCP), the potential difference between the test anodes relative to a saturated calomel reference electrode (SCE), was continuously monitored, commencing from the introduction of the anode into the electrolyte. The OCP plot of OCP versus time up to 60 days is interpreted in terms of the electrode–electrolyte interphase. All the anodes were immersed in 3% NaCl solution at 30 ± 2 °C. The closed circuit potential (CCP) of the test anodes with respect to SCE was continuously monitored when the anode was coupled with a mild steel cathode and the couple was kept immersed in 3% NaCl solution prepared with analytical grade chemicals and distilled water. The CCP variation was monitored for a period of 60 days.

2.3.2 Polarization

The anodes were anodically polarized potentiostatically, against a larger surface area platinum counter electrode. A SCE was the reference electrode. The polarization experiments were repeated to test reproducibility. The anodes were equilibrated in 3% NaCl solution for sufficient time prior to each polarization. A standard potentiostat (BAS, USA) was used.

2.3.3 Self corrosion

The anodes were immersed in 3% NaCl solution for a period of 90 days. The difference in the weight of the coupons before and after immersion was measured after cleaning the anodes using a standard procedure (ASTM G 31). The anodes were kept undisturbed mechanically and electrochemically using suitable supports and complete insulation. The corrosion rate was calculated based on the weight loss data.

2.3.4 Efficiency

The test anode and a steel cathode having 10 times larger surface area was coupled using a copper wire. The cathode had the composition (Fe,C-0.089%, Mn-0.0535%, Si-0.0284%, P-0.043%, S-0.043%, Cr-0.0287%, Ni-0.146%,

Cu-0.043%, Al-0.035%, Ti-0.007%, Sb-0.178%) with dimensions of 10 × 4 × 0.5 cm. The electrical contacts and the top surface of the anodes were insulated. All the similar couples comprising the anodes of determined exposed surface area were immersed in 3% NaCl solution for a period of 90 days. The current was continuously monitored. The weight of the anode before and after immersion was measured after cleaning the anode by a standard procedure (ASTM G 31). From the weight loss data the theoretical current capacity of the anode was calculated. The anode efficiency can be defined as the useful ampere hours charge derived from the anode in practice compared with that theoretically obtainable.

$$Efficiency\,(\%) : \frac{Effective\ current\ capacity \times 100}{Theoretical\ current\ capacity}$$

Parallel experiments were conducted with other electrode couples to ensure reproducibility.

2.3.5 Accelerated electrochemical test

An accelerated electrochemical test was carried out to determine the efficiency of the anodes (ASTM G 97). The tests were carried out by impressing an anodic current density of 1 mA cm^{-2} on the anode coupled with mild steel cathode, for a period of 5 h in the aerated test solution, simulated to ocean water with an initial pH 8.3 according to ASTM D 1141.

The effective current capacity of an anode is the total columbic charge produced by unit mass of the anode as a result of electrochemical dissolution. The theoretical current capacity can be calculated according to Faraday's law. Theoretically Al + 5% Zn alloy has a current capacity of 2,882 Ah kg^{-1}.

2.3.6 Impedance characterization

Electrochemical impedance spectra were carried out using an Auto lab PGSTAT3plus FRA 2 measuring system. An Ag/AgCl, Pt and anodes having 1 cm^2 exposed area were used as reference, counter and working electrodes respectively. The measurements were performed after immersion of the anodes in 3% NaCl solution at 30 ± 2 °C for 2 h in order to obtain steady state conditions.

2.4 Bio-growth

The bio-growth on the anodes was assessed by counting the viable microorganism on the anode surface due to exposure to natural sea water for 1 week. The total viable count (TVC) was determined by a standard plate count method. After 1 week, the biofilm formed on the anode surface was transferred into peptone water. The mixture was shaken for 5 min so that all microorganisms were serially diluted with sterile water to get 10^{-5} dilution. One ml samples were then spread on to zohell marine agar medium. The composition of the zohell marine agar media used was given in the Table 1. The pH and temperature were 7.6 ± 0.2 and 25 °C respectively. The incubation of the plates was carried out for 24–48 h at 37 °C. The colony forming units (CFU) were enumerated and the original counts were calculated from the dilution factor.

$$\text{Microbial counts} = \text{Number of CFU} \times \text{Dilution factor}.$$

Table 1 Chemical composition of the zohell marine agar medium

Chemicals	Concentration/g L^{-1}
Peptone	5.0000
Yeast extract	1.0000
Ferric citrate	0.1000
Sodium chloride	19.4500
Magnesium chloride	8.8000
Sodium sulphate	3.2400
Calcium chloride	1.8000
Potassium chloride	0.5500
Sodium carbonate	0.1600
Potassium bromide	0.0800
Strontium chloride	0.0340
Boric acid	0.0220
Sodium silicate	0.0040
Ammonium nitrate	0.0016
Disodium phosphate	0.0008
Agar	15.0000

3 Results and discussion

3.1 Metallurgical characteristics of the anode

Figure 1a shows the morphology of the Al–Zn anode, and Fig. 1b shows that of the MnO_2-incorporated Al–Zn anode. A significant difference in morphology of the two anodes is apparent. The MnO_2 incorporated anode had uniform morphology with smaller and well defined grains. The grain size and uniform distribution have a large influence on galvanic performance. Generally, anodes with small grains have high current capacity and efficiency [36, 37]. The good wettability and the presence of an optimum amount of MnO_2 in the Al alloy can prevent the precipitation of the composite. No other specific defects like voids, channels and segregations were found. The existence of MnO_2 at the grain boundaries is the likely cause of the metallurgical improvement of the Al–Zn anode. The role of MnO_2 is not confined to the activation process

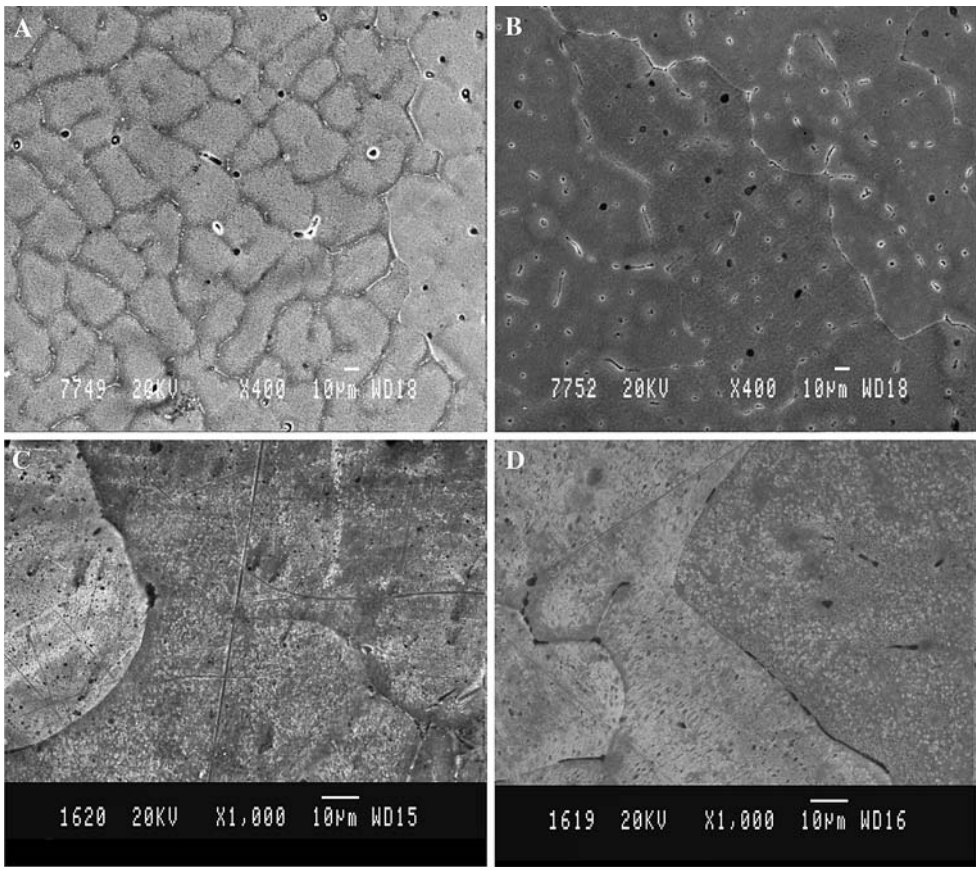

Fig. 1 Surface morphology of (**a**) pure Al + 5% Zn anode, (**b**) MnO_2 incorporated Al + 5% Zn anode, (**c**) and (**d**) respectively at higher magnifications

alone; it also causes substantial reduction in self-corrosion. The presence of MnO_2 in grain boundaries is the cause for suppression of non-columbic loss of grains and hence the self corrosion. Similar inferences were arrived from the SEM micrographs at higher magnifications Fig. 1c, d.

The maximum concentration of the MnO_2 in the sacrificial anodes was limited to 0.5%, since higher amount of the MnO_2 could decrease the energy density of the anode mass. It was also difficult to obtain a homogeneous alloy melt before casting, due to segregation of the MnO_2 in the melt. By means of MnO_2-incorporation, the mechanical properties of the anodes were slightly improved. The hardness of the Al-matrix incorporated with 0.5% MnO_2 was found to be $\sim$52.14 VHN and that of the pure Al–Zn was $\sim$39.92 VHN. The increase in hardness is attributable to dissolution of Mn to Al–Zn alloy [34].

The substantial improvement in the mechanical properties of the Al–Zn anode by MnO_2-incorporation is mainly due to two factors. Firstly, the relatively finer size of the intermetallic layer $MnAl_6$ which results from nucleation provided by numerous alumina particles generated by the reduction of relatively fine MnO_2 particles. Second reason is the reinforcement of the matrix alloy by the formation of in-situ Al_2O_3 within the metal matrix [34, 35].

3.2 Electrochemical evaluations

3.2.1 OCP decay

Figure 2 shows the OCP decay of the galvanic anodes incorporated with different concentrations of MnO_2, in 3% NaCl solution as a function of time. The OCP values were found to lie in the range −0.940 to −0.970 V initially and they shifted to −0.934 to −0.967 V as a result of 2 months immersion. There were fluctuations of potential only at the beginning of the test period and then they became almost stable with a very slight gradual increase in the potential values. This fluctuation in the potential variation versus time is attributable to the non-uniform corrosion of the anode, especially pitting in the case of sacrificial anodes [11].

The anode incorporated with 0.5% MnO_2 exhibited the highest OCP. In this case very little potential fluctuation was observed, also at the beginning of the study and then it became almost stable with a very slight gradual increase. On the other hand the pure Al–Zn anode exhibited a heavy anodic OCP shift. This is attributable to the formation of oxide films on the anode surface leading to ennoblement of the potential [3]. Even though all the MnO_2 incorporated anodes exhibited higher OCP than the pure Al–Zn anode,

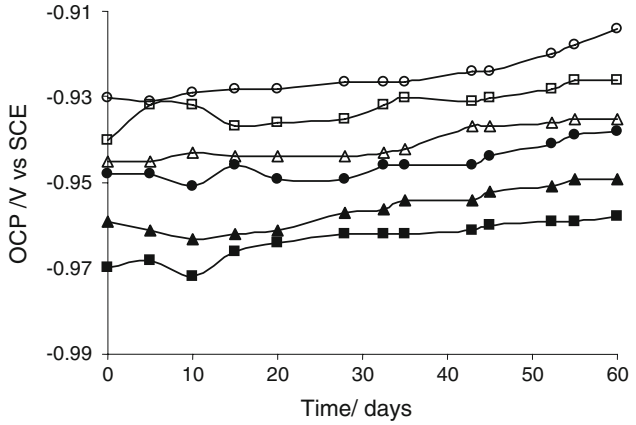

Fig. 2 OCP decay curves of Al + 5% Zn anode with different amounts MnO_2 incorporation. (○) Al + 5% Zn, (□) Al + 5% Zn + 0.05% MnO_2, (Δ) Al + 5% Zn + 0.1% MnO_2, (●) Al + 5% Zn + 0.2% MnO_2, (■) Al + 5% Zn + 0.5% MnO_2, (▲) Al + 5% Zn + 1% MnO_2

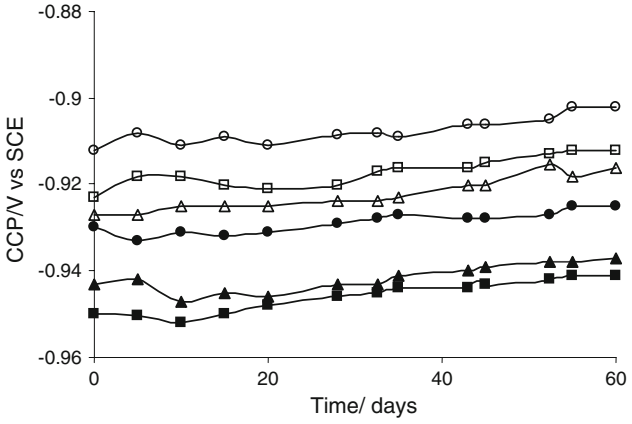

Fig. 3 Variation in CCP of the Al + 5% Zn anode with different amounts of MnO_2 incorporation. (○) Al + 5% Zn, (□) Al + 5% Zn + 0.05% MnO_2, (Δ) Al + 5% Zn + 0.1% MnO_2, (●) Al + 5% Zn + 0.2% MnO_2, (■) Al + 5% Zn + 0.5% MnO_2, (▲) Al + 5% Zn + 1% MnO_2

the best candidate could not be ascertained based on these result alone. In this context, the variation in CCP of the anodes was monitored under the condition of being galvanically coupled with steel cathodes.

3.2.2 CCP variation

Figure 3 shows the CCP variation curves of the Al + 5% Zn alloy anodes incorporated with different concentrations of MnO_2 under a current density of 1 mA cm^{-2}. All the anodes exhibited high cathodic initial CCP values ranging from −0.929 to −0.950 V, which were substantially higher than that of the pure Al–Zn anode and in accordance with the OCP values. The anode incorporated with 0.5% MnO_2, exhibited more active behavior than all other anodes. Generally an active CCP is desirable because a relatively noble potential indicates passivation [38]. Normally CCP values are considered more simulated to actual galvanic exposure, the only difference being the very low currents. Conventionally, CCP values are measured only when the actual galvanic reactions are proceeding. Hence the variation in CCP values could be considered as significant during evaluation of anodic characteristics. In the present case, the galvanic anode incorporated with 0.5% MnO_2 exhibited more active behavior compared to all other anodes.

3.2.3 Anodic polarization

The polarization trends of Al + 5% Zn alloy anode incorporated with different concentrations of MnO_2 are shown in Fig. 4. The polarization curve of the Al + 5% Zn alloy sacrificial anode was characterized by a broad passive region within the entire current range. This is attributable to the formation of protective oxide films on the aluminum

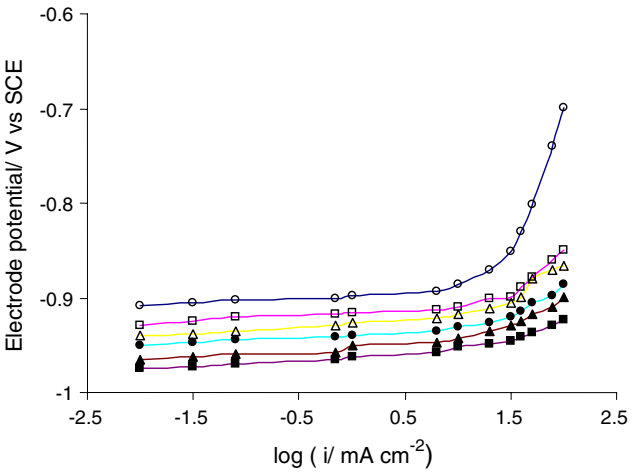

Fig. 4 Anodic polarization behavior of Al + 5% Zn anode with different amounts MnO_2 incorporation. (○) Al + 5% Zn, (□) Al + 5% Zn + 0.05% MnO_2, (Δ) Al + 5% Zn + 0.1% MnO_2, (●) Al + 5% Zn + 0.2% MnO_2, (■) Al + 5% Zn + 0.5% MnO_2 (▲) Al + 5% Zn + 1% MnO_2

surface. The 0.5% MnO_2 incorporated anode exhibited the least polarization among all the anodes studied. Higher and lower amounts of MnO_2 caused high polarization revealing that the optimum and critical concentration of the MnO_2 is 0.5%. Addition of MnO_2 to the alloy anodes produces such metallurgical characteristics that the anode surface forms an efficient double layer interface with the electrolyte resulting in more cathodic polarization.

3.2.4 Self corrosion

The overall galvanic performance of the MnO_2-incorporated Al–Zn alloy sacrificial anodes are compared in Table 2. All the anodes containing MnO_2 exhibit better galvanic

performance such as more cathodic OCP and CCP, high galvanic efficiency and low self corrosion. The major drawbacks of the Al–Zn sacrificial anodes are non-coulumbic loss and low galvanic efficiency. In the present work, self corrosion of the anode was determined to assess the non-coulumbic loss. From Table 2 it is clear that all the MnO_2 incorporated anodes exhibit low self corrosion for a period of 3 months in 3% NaCl solution, when compared with pure Al–Zn alloy anode. The self corrosion value of pure Al–Zn alloy sacrificial anode is 10.860×10^{-6} g cm^{-2} h^{-1} and that of MnO_2-incorporated anodes are in the range 8.215×10^{-6}–7.129×10^{-6} g cm^{-2} h^{-1}. Among all the MnO_2-incorporated anodes, 0.5% MnO_2 exhibited the least value, which is in accordance with the results of OCP decay and polarization studies. The reduction in self corrosion values may be attributed to reduction in grain boundary corrosion due to better grain refinement [20]. Thus it is clear that the inclusion of MnO_2 suppresses the self corrosion of Al–Zn sacrificial anodes.

3.2.5 *Galvanic efficiency*

The galvanic efficiency values of anodes with different concentrations of MnO_2 are given in Table 2. The galvanic efficiency and self corrosion values are in good agreement for all the anodes. The pure Al–Zn anode exhibited an efficiency of just 58.5%. Aluminum and aluminum alloys generally suffer from pitting and localized corrosion in 3% NaCl solutions. This is the main cause of low galvanic efficiency and high self-corrosion of aluminum anodes [39]. On the other hand the 0.5% MnO_2 incorporated anode exhibited remarkably high efficiency, around 80%, suggesting uniform anode dissolution. The incorporation of higher concentrations of MnO_2 caused a drastic decrease in the efficiency and hence the incorporation of higher concentrations of MnO_2 was not further considered.

3.2.6 *Accelerated electrochemical test*

With reference to 0.5% MnO_2 incorporation as the best and optimum, the galvanic efficiency of other anodes incorporated with different concentrations of MnO_2 are compared in Table 2. The efficiency was determined by an accelerated test involving the impression of an anodic current density of 1 mA cm^{-2} on the anode coupled with a mild steel cathode, for a period of 5 h. The 0.5% MnO_2 anode showed higher efficiency than that of other anodes. Theoretically, uniform anode dissolution will give maximum efficiency. Either secondary cathodic reaction on the surface interface and/or mechanical grain loss due to local macro/micro corrosion cells will reduce anode efficiency. With the addition of higher concentrations of MnO_2, heterogeneity in the Al–Zn alloy melt was noticed. The performance of the anode under practical exposure conditions would be still better as the current density would be relatively low under such circumstances.

3.2.7 *Impedance analysis*

In the present work, the impedance technique was used as a basis for a comparative study to show the corrosion behavior of the anodes viz; Al + 5% Zn and Al + 5% Zn + 0.5% MnO_2. The EIS were recorded only after the anodes attained steady state i.e., after 2 h in 3% NaCl. The analysis was made within the frequency range 1–10 MHz, with reference to OCP. The Bode and Nyquist plots of the Al + 5% Zn and Al + 5% Zn + 0.5% MnO_2 anodes are shown in Fig. 5a, b respectively. At the high frequency limit, the impedance 'z' was dominated by the solution resistance (Rs) while at the very low frequency limit; the impedance approached the sum of solution and polarization resistance (Rp). The impedance spectra showed a depression in the modulus of impedance, |Z| obtained at lower frequencies corresponding to a Al + 5% Zn alloy anode revealing pitting behavior [23].The Al + 5% Zn + 0.5% MnO_2 anode exhibited significantly lower resistivity when compared with Al + 5% Zn, a favorable criterion for a good sacrificial anode. The Rp, CPE/F and n values of the alloy and the matrix sacrificial anodes were 83.56, 9.257×10^{-9}, 1.251 and 74.848, 1.180×10^{-8}, 1.312 respectively. The variation in the polarization resistance may be attributed to the MnO_2 induced activation of the sacrificial anodes.

Table 2 A comparison of the galvanic performance of the MnO_2 incorporated Al + 5% Zn alloy sacrificial anode [Electrolyte: 3% NaCl]

Sl. No.	Amount of MnO_2 (wt.%)	O.C.P. versus SCE (V)	C.C.P. at i = 1 mA cm^{-2} (V)	Self-corrosion $\times 10^{-6}$ (g cm^{-2} h^{-1})	Efficiency (%)	Efficiency (i = 1 mA cm^{-2}) (%)
1	–	−0.930	−0.912	10.860	58.5	25
2	0.05	−0.940	−0.923	8.215	60.0	28
3	0.1	−0.945	−0.927	8.152	61.0	30
4	0.2	−0.948	−0.930	7.861	63.0	32
5	0.5	−0.970	−0.950	7.159	80.0	66
6	1.0	−0.959	−0.943	7.299	75.0	59

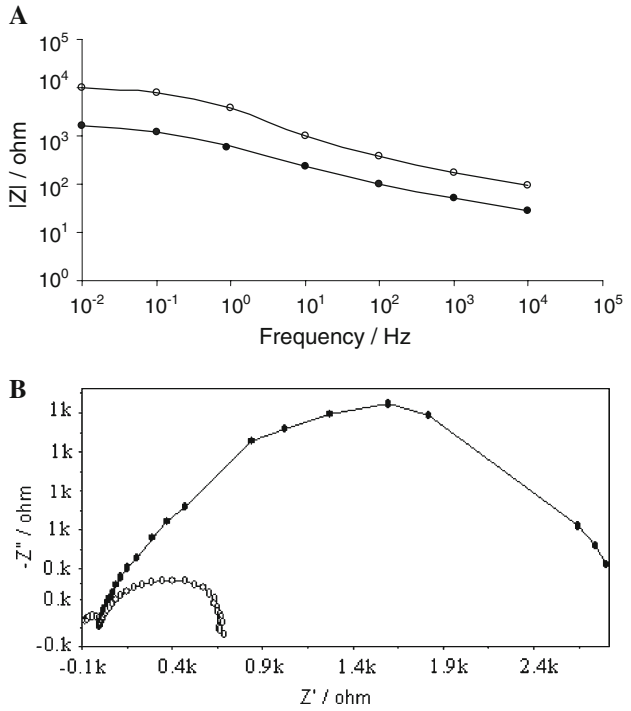

Fig. 5 (**a**) Bode plots of Al + 5% Zn anode with different amounts MnO_2 incorporation. (○) Al + 5% Zn, (●) Al + 5% Zn + 0.5% MnO_2, (**b**) Nyquist plots of (●) Al + 5% Zn, (○) Al + 5% Zn + 0.5% MnO_2

3.3 Bio-growth

The number of viable micro organisms observed by a standard plate count method after incubation is shown in Fig. 6. The number of cell colonies attached to the pure Al–Zn anode was approximately 2360 CFU cm^{-2} while the MnO_2 incorporated anodes exhibited cell colonies in the range 2,160–1,290 CFU cm^{-2}. With increasing MnO_2 concentration there was a significant reduction in bacterial adhesion. Thus, MnO_2 incorporation results in effective suppression of biofouling and the possibility of microbially induced corrosion.

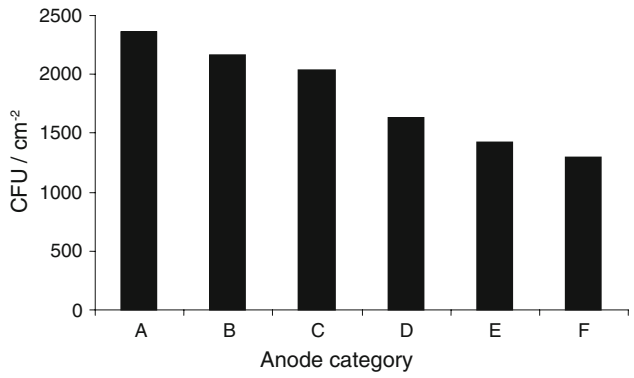

Fig. 6 Comparison of the numbers of cell colonies attached to Al + 5% Zn anode with different amounts MnO_2 incorporation. (A) Al + 5% Zn, (B) Al + 5% Zn + 0.05% MnO_2, (C) Al + 5% Zn + 0.1% MnO_2, (D) Al + 5% Zn + 0.2% MnO_2, (E) Al + 5% Zn + 0.5% MnO_2, (F) Al + 5% Zn + 1% MnO_2

4 Conclusions

The optimum quantity of MnO_2 incorporation facilitated effective activation of the anodes. The metallurgical characteristics of the anodes were improved substantially by means of MnO_2 incorporation leading to a substantial reduction in self corrosion. The galvanic performance of the anodes was improved significantly by incorporating MnO_2. This led to a significant increase in efficiency from 58.5 to 80%. The anode incorporated with 0.5% MnO_2 exhibited very low polarization during galvanic exposure as predicted based on the results of anodic polarization by impressed current. It also exhibited a high and steady negative OCP and CCP. The incorporation of the MnO_2 in optimum quantity was crucial as other combinations had negligible or even adverse effects. These promising anodes are associated with further advantages in terms of low cost, easy development, tolerance in aggressive media and bio-resistance.

Acknowledgements The authors are grateful to the Head of the Department of Chemistry, University of Kerala, for his kind assistance.

References

1. Gonzalez C, Alvarez O, Genesca J, Juarez JA (2003) Metall Mater Trans A 34A:2991
2. Bruzzone G, Barbucci A, Cerisola G (1997) J Alloys Compd 247:210
3. Abdein SZ, Endres F (2004) J Appl Electrochem 34:1071
4. Ponchel BM, Horst RL (1968) Mater Protect 7:38
5. Pourbiax M (1966) Atlas of electrochemical equilibria in aqueous solutions. Pergamon, Oxford, p 171
6. Bessone JB (2006) Corros Sci 48:4243
7. Shibli SMA, Gireesh VS (2003) Appl Surf Sci 219:203
8. Guruppa I, Karnik JA (1996) Corros Prev Cont 43:77
9. Venugopal A, Raja VS (1996) Br Corros J 31:318
10. Sato F, Newmann RC (1998) Corrosion 54:955
11. Sina H, Emamy M, Saremi M, Keyveni A, Mahta M, Campbell J (2006) Mater Sci Eng A 431:263
12. Shibli SMA, George S (2007) Appl Surf Sci 253:7510
13. Muller JC, Galvele JR (1977) Corros Sci 17:995
14. Lyublinski EY (1973) Electrochimiya 9:491
15. Maity PC, Chakraborty PN, Panigrahi SC (1994) Mater Lett 20:93
16. Kamat SV, Hirth JP, Mehrabin R (1989) Acta Metall 37:2395
17. Ravichandran MV, Krishna Prasad R, Dwarakadasa ES (1992) J Mater Sci Lett 11:452
18. Ragunathan SV, Ioannidis EK, Sheppard T (1991) J Mater Sci 26:985
19. Kamat SV, Rollet AD, Hirth JP (1991) Scrip Metall Mater 25:27
20. Shibli SMA, Jabeera B, Manu R (2007) Mater Lett 61:3000

21. Kaji T, Hattori H, Hishikura M, Takeda Y (1999) Japanese Patent 137676
22. Yamada T, Ogiwara Y, Doko T (2000) Japanese Patent 144290
23. Ashraf PM, Shibli SMA (2007) Electrochem Comm 9:443
24. Torralba JM, Costab CE, Velasco F (2003) J Mater Process Technol 13:203
25. Ghosh A, Chatterjee S, Sankar BK (1999) Trans Powder Metall Assoc India 26:201
26. Jabeera B, Anirudhan TS, Shibli SMA (2005) J New Mater Electrochem Syst 8:291
27. Bruke LD, Murphy OJ (1980) J Electroanal Chem 112:39
28. Geuard WA, Steck BCH (1978) J Appl Electrochem 8:417
29. Donne SW, Kennedy JH (2004) J Appl Electrochem 34:159
30. Lima FHB, Calegaro ML, Ticianelli EA (2006) J Electroanal Chem 590:152
31. Chou S, Cheng F, Chen J (2006) J Power Sour 162:727
32. Pang SC, Anderson MA, Chapmann TW (2000) J Electrochem Soc 147:4444
33. Prasad KR, Miura N (2004) Electrochem Comm 6:1004
34. Hamid AA, Ghosh PK, Jain SC, Ray S (2005) Metall Mater Trans A 36:2211
35. Hamid AA, Ghosh PK, Jain SC, Ray S (2006) Wear 260:368
36. Shibli SMA, Dilimon VS, Asha M (2007) J Appl Electrochem 37:1015
37. Qi C, Guo Z, Zhang H, Qiu Y, Zhang X (1997) Fushi Kexue Yu Fanghu Jishu 9:231
38. Talavera MA, Valdez S, Juarez JA, Mena B, Gnesca J (2002) J Appl Electrochem 32:897
39. Salinas DR, Garcia SG, Bessone JB (1999) J Appl Electrochem 29:1063